Structure of Organic/Inorganic Interface in Assembled Materials Comprising Molecular Components. Crystal Structure of the Sensitizer Bis[(4,4′-carboxy-2,2′-bipyridine)(thiocyanato)]ruthenium(II)

V. Shklover,*,† Yu. E. Ovchinnikov,† L. S. Braginsky,† S. M. Zakeeruddin,‡ and M. Grätzel‡

Laboratory of Crystallography, Swiss Federal Institute of Technology, CH-8092 Zürich, Switzerland, and Institute of Photonics and Interfaces, Department of Chemistry, Swiss Federal Institute of Technology, CH-1015 Lausanne, Switzerland

Received April 22, 1998. Revised Manuscript Received July 8, 1998

Structural data have been obtained for the photosensitizer bis[(4,4′-carboxy-2,2′-bipyridine)-(thiocyanato)]ruthenium(II) (**1**) via X-ray diffraction analysis. Crystals of **1** are triclinic, $a = 11.4663(4)$ Å, $b = 12.5897(5)$ Å, $c = 18.9329(7)$ Å, $\alpha = 75.238(2)°$, $\beta = 89.611(2)°$, $\gamma = 66.446(2)°$, space group $P\bar{1}$, $Z = 2$, refinement to $R = 0.0809$, $R_w = 0.0950$ for 4045 observed reflections. Structural models of sensitizer molecules anchoring to the TiO_2 anatase surface and models of close-packed sensitizer monolayers with different anchoring types have been built by using experimental geometry of known organic Ti complexes and the X-ray structure of sensitizer **1**. On the basis of a simple one-dimensional tight-binding model, it was suggested that possible modifications of TiO_2/sensitizer interface could enhance interfacial transparency for injected electrons.

Introduction

A new type of photovoltaic cell was reported recently based on spectral sensitization of thin nanocrystalline TiO_2 (anatase) films by Ru polypyridine complex chromophores.[1] Generally, the interfacial electron transfer from a photoexcited state of the chromophore into the conduction band of the semiconductor depends on a number of factors. The atomic structure of the interface is highly important, since some of its general characteristics can affect directly on the electron transfer: (i) coherence of the sensitizer monolayer and semiconductor surface, (ii) surface density of the sensitizer monolayer, and (iii) number of bonds between the sensitizer molecule and semiconductor surface. The first feature is displayed, for example, in epitaxial multilayered all-oxide materials, wherein better crystallographic correspondence of the layers provides better conductivity.[2] The importance of the two other characteristics mentioned for the electron transfer are evident. Earlier we developed a one-dimensional tight-binding model[3] to explain the electron transport across the sensitizer/semoconductor interface. This was a generalization of the known model for "sharp" semiconductor/semiconductor heterojunctions.[4] This model allowed us to formulate a criterion for interface transparency and for "sharpness" of the interface.

There is a lack of experimental data on interface structure at the atomic level due to difficulties in using direct and diffraction methods (AFM, LEED) to determine the structure of the sensitizer monolayer. The study of the crystal surface of sensitizers or the substrate itself is not a problem.[5−7] Hence possible modes of binding of the photosensitizer on the substrate surface can be analyzed via simulation using the known structural data of the components involved (sensitizer and the substrate). Possible future results of indirect methods, such as photoelectron diffraction and grazing X-ray scattering, may be interpreted only in terms of structural models built independently.

We report in this paper the first results of molecular modeling of the sensitizer monolayer on a TiO_2 anatase surface. To build these models, we used the known crystal structure of anatase and our results on the X-ray crystal structure determination of the sensitizer bis-[(4,4′-carboxy-2,2′-bipyridine)(thiocyanato)]ruthenium-(II) (**1**). On the basis of a simple one-dimensional tight-binding model, suggestions are made for the possible modification of the TiO_2/sensitizer interface with the aim to improve its transmittance for electrons.

* To whom correspondence should be addressed.
† Laboratory of Crystallography.
‡ Institute of Photonics and Interfaces.

(1) Grätzel, M. *Comments Inorg. Chem.* **1991**, *12*, 93.
(2) Suzuki, M.; Ami, T. *Mater. Sci. Eng.* **1996**, *B41*, 166.
(3) Braginsky, L.; Shklover, V. *J. Sol. State Commun.* **1998**, *105*, 701.
(4) Niles, D. W.; Margaritondo, G. In *Materials Interfaces. Atomic Level Structure and Properties;* Wolf, D., Yip, S., Eds.; Chapman and Hall: New York, 1992; p 592.
(5) Pechy, P.; Rotzinger, F.; Nazeeruddin, M. K.; Kohle, O.; Zakeeruddin, S. M.; Humphry-Baker, R.; Grätzel, M. *Chem. Commun.* **1995**, 65.
(6) Shklover, V.; Nazeeruddin, M.-K.; Zakeeruddin, S. M.; Barbe, C.; Kay, A.; Haibach, T.; Steurer, W.; Hermann, R.; Nissen, H.-U.; Grätzel, M. *Chem. Mater.* **1997**, *9*, 430.
(7) Shklover, V.; Haibach, T.; Bolliger, B.; Hochstrasser, M.; Erbudak, M.; Zakeeruddin, S. M.; Nazeeruddin, Md. K.; Grätzel, M. *J. Solid State Chem.* **1997**, *132*, 60.

S0897-4756(98)00303-2 CCC: $15.00
Published on Web 09/03/1998

Table 1. Experimental Details of X-ray Structure Study for the Sensitizer 1 ($Ru(dcbbpy)_2(NCS)_2 \cdot 5OS(CH_3)_2$)

formula weight	1096.28
crystal color, habit	dark red, thin plate
crystal dimensions (mm)	0.26 × 0.10 × 0.02
crystal system	triclinic
space group	$P\bar{1}$
lattice parameters	
a (Å)	11.4663(4)
b (Å)	12.5897(5)
c (Å)	18.9329(7)
α (deg)	75.238(2)
β (deg)	89.611(2)
γ (deg)	66.446(2)
V (Å^3)	2408.7(2)
Z	2
density calc (g cm^{-3})	1.511
absorption coefficient	
μ (Mo Kα) (mm^{-1})	0.69
F(000)	1128
T (K)	243(2)
reflections measured	8406
independent reflections, R_{int}	3768
observed reflections, $F > 6\sigma(F)$, used in refinement[a]	4045
no. of refined parameters	493
residuals R, R_w	0.0809, 0.0950
reflections/parameters ratio	8.2
goodness of fit	1.08

[a] Averaging of equivalents was not applied.

Experimental Section

Synthesis of the sensitizer **1** was reported earlier;[8] single crystals for X-ray study have been obtained on slow evaporation of a DMSO solution of **1**.

X-ray Structure Study of Complex 1. The data collection for a single crystal **1** was performed at 243 K on Siemens SMART PLATFORM with CCD detector, using Mo Kα radiation, graphite monochromator, and the ω-scan technique with an exposure time of 120 s/frame. Other experimental details and results of the structure refinement are depicted in Table 1. The H atoms were not localized, but in bipyridyl moieties they were placed in calculated positions and refined as "riding" atoms with fixed C−H distances and isotropic temperature factors $U = 0.08$ Å^2. The O and C atoms of solvate DMSO molecules were refined isotropically. Because of a considerable deficit of reflections, all the sphere was involved in refinement. Nevertheless, there were no constrains used for the potentially equivalent geometrical parameters of the structure (like S−C bonds in SCN groups and so on). The coordinates of nonhydrogen atoms are listed in Table 2. The SHELXTL PLUS[9] suite of programs was used for data reduction, structure solution, and refinement.

Scanning Electron Microscopy (SEM). The nanocrystalline colloidal powders of TiO_2 anatase were examined at 30 kV accelerating voltage in a Hitachi S-900 "in-lens" field-emission scanning electron microscope with a standard Everhard-Thornley SE detector and YAG-type BSE detector at the Laboratory of Electron Microscopy I of the Swiss Federal Institute of Technology (ETH-Zürich). Digital Micrograph 2.1 software was used for the digital processing of SEM images.[10]

High-Resolution Transmission Electron Microscopy. The HRTEM study of the TiO_2 anatase single crystals coated with sensitizer **1** was performed at 300 kV on Philips CM 30 ST transmission electron microscope equipped with a detector for energy-dispersive X-ray spectrometry (EDX) and a STEM attachment.

Table 2. Atomic Coordinates (× 10^4) and Equivalent Displacement Parameters U_{eq} (Å^2 × 10^3) of Non-Hydrogen Atoms in the Crystal 1

Atom	x	y	z	U_{eq}[a]
Ru(1)	1878(1)	10893(2)	2997(1)	28(1)
S(1)	305(6)	14644(6)	1081(3)	97(2)
S(2)	5174(5)	12186(6)	3407(3)	73(2)
O(1)	−3341(10)	9604(14)	2272(7)	101(3)
O(2)	−2499(12)	9584(17)	1226(8)	126(3)
O(3)	3369(11)	7760(13)	322(6)	78(3)
O(4)	5100(11)	8138(13)	343(7)	82(3)
O(5)	3984(12)	5427(10)	5823(7)	78(3)
O(6)	2684(10)	6752(11)	6375(6)	62(3)
O(7)	−445(11)	12122(10)	6233(6)	64(3)
O(8)	−891(16)	14018(13)	5602(7)	118(3)
N(11)	415(10)	10537(12)	2673(7)	31(3)
N(21)	2700(10)	9997(11)	2247(6)	27(3)
N(31)	2447(10)	9388(12)	3883(7)	33(3)
N(41)	1056(10)	11633(12)	3798(7)	36(3)
N(51)	1171(11)	12484(13)	2182(7)	35(3)
N(61)	3411(11)	11244(13)	3218(6)	41(3)
C(12)	630(12)	9958(14)	2180(8)	30(3)
C(13)	−248(14)	9618(15)	1905(8)	44(3)
C(14)	−1511(13)	10015(15)	2124(9)	51(3)
C(15)	−1702(13)	10582(14)	2656(8)	37(3)
C(16)	−738(13)	10925(14)	2916(8)	39(3)
C(17)	−2504(14)	9668(15)	1854(11)	54(3)
C(22)	1905(13)	9595(14)	1898(7)	28(3)
C(23)	2362(11)	9010(14)	1385(7)	27(3)
C(24)	3542(14)	8836(15)	1165(9)	47(3)
C(25)	4281(13)	9278(15)	1456(9)	43(3)
C(26)	3858(13)	9822(15)	2005(9)	42(3)
C(27)	4013(14)	8248(14)	553(9)	38(3)
C(32)	1999(12)	9614(13)	4530(8)	26(3)
C(33)	2316(12)	8650(13)	5150(8)	25(3)
C(34)	3021(13)	7494(14)	5128(8)	29(3)
C(35)	3482(13)	7262(16)	4489(9)	47(3)
C(36)	3124(13)	8257(14)	3854(9)	34(3)
C(37)	3230(15)	6512(14)	5853(10)	41(3)
C(42)	1259(12)	10869(13)	4498(8)	19(3)
C(43)	756(12)	11306(14)	5084(8)	28(3)
C(44)	82(13)	12546(15)	5013(9)	36(3)
C(45)	−80(13)	13293(15)	4316(9)	46(3)
C(46)	414(13)	12825(15)	3722(8)	33(3)
C(47)	−440(14)	12891(16)	5666(11)	53(3)
C(81)	794(15)	13398(18)	1729(9)	58(3)
C(82)	4105(14)	11617(16)	3301(8)	45(3)
		Solvate Molecules		
S(3)	−3722(7)	8213(10)	4022(4)	172(3)
O(301)[b]	−2718(15)	8603(16)	3680(9)	144(3)
C(301)[b]	−4247(25)	8965(26)	4771(17)	190(4)
C(302)[b]	−2793(23)	6845(25)	4416(15)	161(4)
S(4)	5477(6)	6216(7)	−907(4)	112(2)
O(401)[b]	4164(12)	6662(13)	−642(7)	92(3)
C(401)[b]	5652(15)	7586(17)	−1353(9)	68(3)
C(402)[b]	6606(19)	5658(20)	−182(12)	102(4)
S(5)	2617(9)	4519(9)	7429(6)	186(3)
O(501)[b]	4032(16)	3965(17)	7051(9)	155(3)
C(501)[b]	3095(20)	4875(22)	8203(13)	130(4)
C(502)[b]	2316(23)	3380(25)	7898(16)	165(4)
S(6)	−2548(9)	14200(8)	7060(6)	165(3)
O(601)[b]	−1696(16)	12878(18)	7202(10)	153(3)
C(601)[b]	−3310(24)	14285(26)	7865(16)	184(4)
C(602)[b]	−1706(16)	14928(18)	7158(10)	75(3)
S(7)	−365(8)	8456(9)	37(5)	153(3)
O(701)[b]	217(18)	7906(19)	772(11)	173(4)
C(701)[b]	755(19)	7591(21)	−461(12)	115(4)
C(702)[b]	−1643(17)	7928(18)	−8(10)	86(3)

[a] Equivalent isotropic coefficients U_{eq} defined as one-third of the trace of the orthogonalized U_{ij} tensor. [b] Isotropic refinement.

Results and Discussion

Structure of TiO_2 Anatase (101) Surface. The subject of our structural consideration is the (101) anatase surface, because it presents the major part of

(8) Nazeeruddin, M. K.; Kay, A.; Rodicio, J.; Humphrey-Baker, R.; Muller, E.; Liska, P.; Vlachopoulos, N.; Grätzel, M. *J. Am. Chem. Soc.* **1993**, *115*, 6382.

(9) Sheldrick, G. M. *SHELXTL PLUS. VAX/VMS Version*; Siemens Analytical X-ray Instruments Inc., Madison, WI, 1990.

(10) *Digital Micrograph. Users Guide, 1992−1994*; Gatan, Inc., 6678 Owens Drive, Pleasonton, CA.

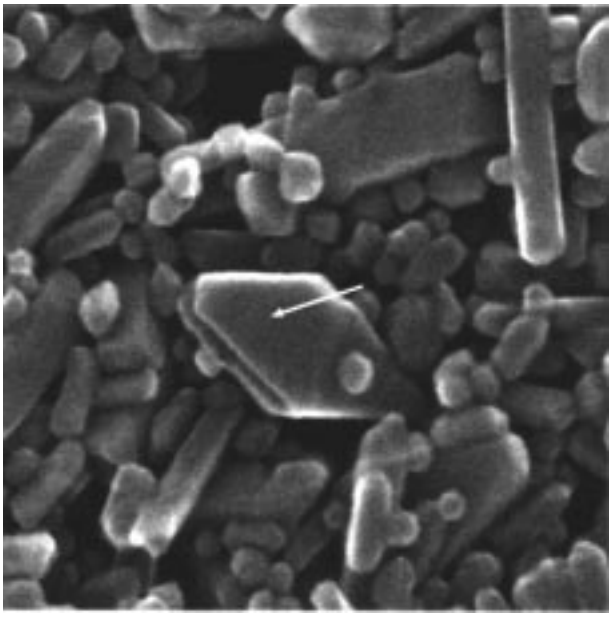

Figure 1. SEM pattern of the nanocrystalline TiO_2 anatase thin film with a thickness of 7.5 μm (top view), showing three main morphologies of anatase nanoparticles: square bipyramidal (indicated with the arrow), pseudocubic, and stablike. According to HRTEM measurements,[6] the (101) faces of anatase nanoparticles of all three morphologies are exposed mostly, the next exposed faces are (100) and (001). The patterns' size is 210 nm.

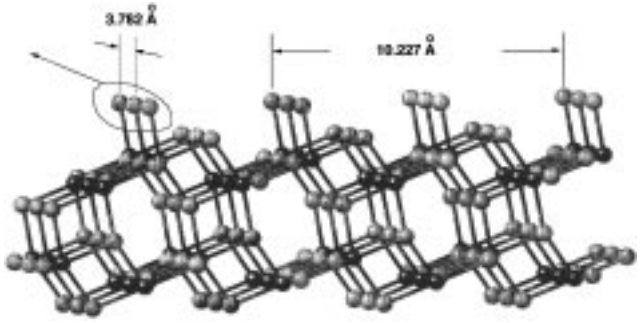

Figure 2. Anatase (101) surface, side view. The protruded rows of terminal O atoms must be removed for stoichiometry and represent the chemisorption sites. Dimensions of the rectangular centered surface cell are presented. This and all the rest of the figures were produced with Cerius[2] software (Molecular Simulations Inc., 1994).

exposed area for anatase nanocrystals.[11] The (101) surfaces are also mostly exposed in nanocrystalline TiO_2 anatase thin films, which we are using for the dye coating in solar cells (Figure 1). The cleavage of this surface shown in Figure 2 seems to be most favorable from different points of view. For a charge balance the surface must be stoichiometric, so if the protruded rows of O atoms indicating in Figure 5 are removed, the rows of pentacoordinated Ti atoms (Ti^{V}) appear. Along with them, the rows of two-bonded O atoms are formed on the surface (in the bulk TiO_2 all the oxygens are three-bonded). Other possible cases of cleavage either destroy the stoichiometry or produce a considerable quantity of four-coordinated Ti^{IV} atoms and terminal oxygens. Obviously, the presence of a lot of "undercoordinated" atoms on a surface increases its energy. Of course, a real surface has many defects of different types; however, they do not define surface structure of sufficiently pure monocrystals.

One more advantage of the suggested cleavage concerns a possible surface reconstruction. If it takes place, displacements of atoms, especially along the surface,[12] can devaluate the models which are built using crystallographic geometry. However, such displacements for the surface under consideration are very likely to be insignificant.

Indeed, Ti^{IV} atoms lost only one coordination bond and their positions in the "microfacets" inclining to the surface (Figure 2) retain rigidity. On the other hand, Ti^{IV}−O bonds involving two-bonded oxygens differ very little from the bulk distances as structures of organometallic complexes show, hence, the shifts of surface O atoms must be small, too. All that allows us to neglect possible differences between bulk and surface geometry, although a strict crystallographic symmetry is certainly distorted on the surface.

Removed rows of O atoms indicated in Figure 2 present the positions which oxygens of sensitizer molecules can occupy without any steric strain. These positions (chemisorption sites) form the same lattice as the corresponding Ti^{IV} atoms do, i.e., rectangular centered lattice having dimensions $a = 3.782$ Å (equals to a or b of the anatase crystal) and $b = 10.227$ Å (corresponds to the $\mathbf{a} + \mathbf{c}$ vector of the crystal). In the projection normal to the surface, these sites are arranged as parallel rows with the spacing $b/2 = 5.11$ Å and shifting along **a** by $a/2$ per one row. Thus the shortest distances between adsorption sites are 3.78 (a), 5.45 (along $\mathbf{a} + \mathbf{b}/2$), 7.56 ($2a$), 7.64 (along $3/2\mathbf{a} + \mathbf{b}/2$), and 10.23 Å ($b$).

Molecular and Crystal Structure of Sensitizer 1. The molecular structure of **1** in the crystal (Figure 3) corresponds well to the structure of an ethylated precursor **2** which was determined earlier by us.[6] Carboxylate groups do not hold the shaded conformation, one of them, viz. C(17)−O(1)−O(2), is skewed up to 30° from the ideal orientation, which is coplanar to the corresponding aryl moiety. The high temperature factors of the oxygen atoms also indicate the mobility of these groups. Despite a rather low accuracy of the structure and indeterminated positions of H atoms, strong H-bonds with solvate DMSO molecules are clearly seen from C(O)O···O(DMSO) distances of 2.47−2.61 Å. These interactions, however, have little effect on COO rotational oscillations, possibly because the DMSO molecules are also very mobile, as could be seen from their high temperature factors.

The approximate C_2 symmetry of the molecule **1** about the bisector line of N(11)−Ru(1)−N(31) and N(51)−Ru(1)−N(61) bond angles should be noted. In the projection along this axis the molecule as a two-dimensional object has an inversion center (Ru atom). Below is shown the influence of this symmetry on the symmetry of possible packings in the sensitizer monolayer (S-monolayer).

Earlier[6] we used the molecular structure of the precursor **2** to find out characteristic geometrical parameters playing an essential role in the adsorption

(11) Spoto, G.; Morterra, C.; Marchese, L.; Orio, L.; Zecchina, A. *Vacuum* **1990**, *41*, 37.

(12) Zajonz, H.; Meyerheim, H. L.; Moritz, W.; Wolf, D.; Schulz, H. *HASYLAB Annual Report II* **1995**, II-235.

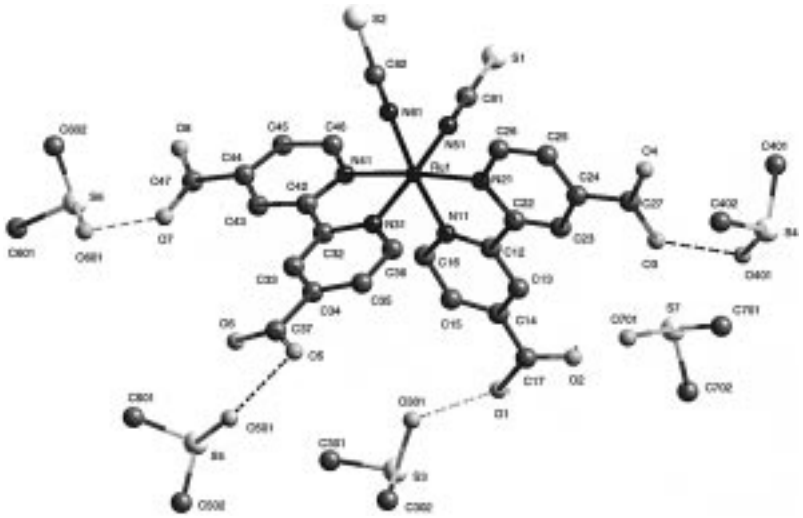

Figure 3. Molecular structure of Ru complex **1** in the crystal. H-bonds with DMSO molecules are shown by dashed lines. H-atoms are omitted.

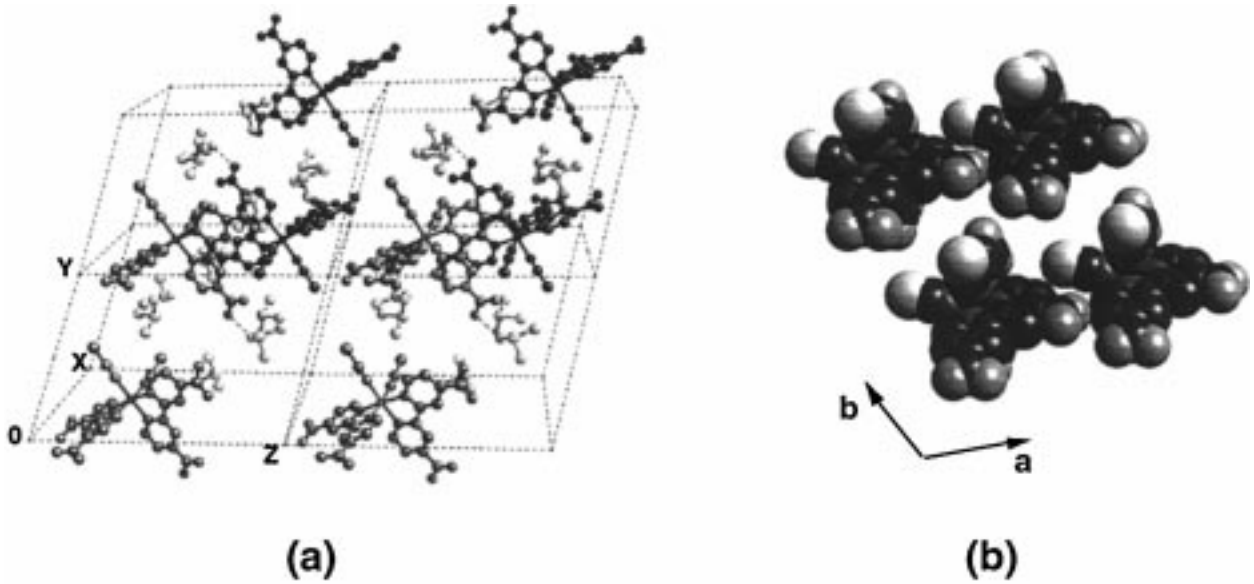

Figure 4. Molecular packing in the crystal **1**: (a) contents of four unit cells displaying layered structure of the crystal; molecules in the far plane are blackened, (b) four closest molecules in the ab plane with their contacting (van der Waals) surfaces.

process. Primarily, these are interatomic distances between O atoms which can be involved simultaneously in interaction with the semiconductor surface. Generally, such intramolecular distances are not too different for **1** and **2**; however, two of them, viz. O(1)···O(6) and O(2)···O(5) (Figure 3), differ by more than 1 Å: 9.8 Å (**1**) vs 10.9 Å (**2**). As one can see from the considerations below, such a difference is enough for making quite wrong conclusions about the possibility of a given anchoring type. So, it is well to bear in mind that a precursor structure, even relatively rigid, may well confuse the process of model building.

A similar assertion should be made concerning the use of sensitizer crystal structure **1** for some prognosis about molecular packing in the S-monolayer. The packing in the crystal **1** (Figure 4) is very friable because of a high concentration of DMSO molecules, and molecules **1**, in fact, do not contact each other. Of course, some features can be traced through different structures containing molecules of a given type, e.g. the similarity of molecular orientations, the coplanarity of bipyridyl planes in neighboring molecules, and H-bonding.

Possible Arrangements of S-Molecules on the (101) Anatase Surface. The simplest and also the initial attaching of the sensitizer molecule to the anatase surface is a single-bond type (A-type, Figure 5a). Although an anchoring oxygen may belong to different COO groups (further we will discriminate these groups as corresponding to the "long" molecular axis C(27)··· Ru(1)···C(47) and "short" axes C(17)···Ru(1)···S(2) and C(37)···Ru(1)···S(1)), the main feature of A-type anchoring is the great rotational freedom of the molecule, resulting from rather large angular intervals of rotation about three single bonds Ti−O, O−C, and C−C. In fact, taking into account also the well-known "softness" of valent angles at Ti and O atoms, the molecule may easily accept almost any orientation, limited by the anatase surface only.

The rotation mentioned leads to immediate capture of another O atom of the COO group by a neighboring Ti atom, being by 3.78 Å from the first, and thus anchoring types B and C appear (Figure 5b). The B or C denote the COO group being on the short molecular axes or on the long axis, respectively. Of course, the

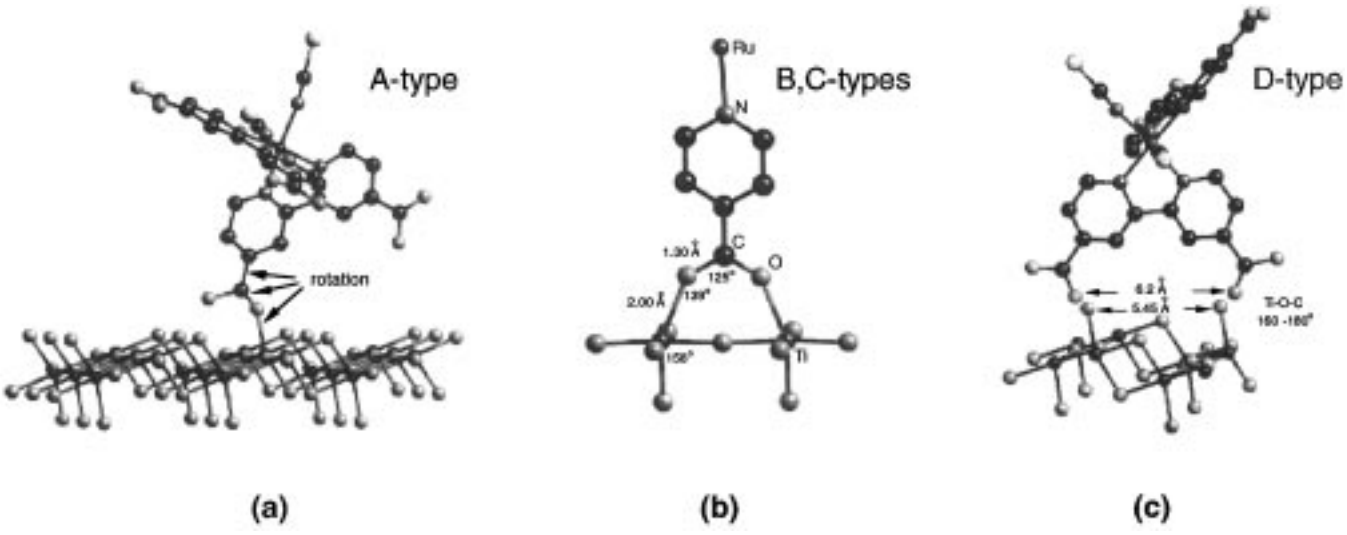

Figure 5. Possible one- and two-bond anchoring types for molecule **1** on the (101) surface of anatase (details are in the text).

anchoring geometry shown in Figure 5b is a model geometry. Such parameters as the Ti−O and C−O bond lengths may be somewhat different, but hardly vary by more than 0.05 Å. In the last available version of CSD,[13] we found 71 fragments Ti−O−C−O−Ti containing octahedral Ti atoms mainly with an oxygen and nitrogen environment. Average parameters of the bridging are Ti−O, 2.03 Å; O−C, 1.26 Å; Ti−O−C, 135°; O−C−O, 124°. The wide scattering of the CSD data should be noted, e.g. such bond lengths as ca. 1.20 Å for C−O may be attributed to the low accuracy of the corresponding structures and/or the significant thermal oscillations of the bridge. In view of these facts, the suggested geometry of the "fork" anchoring (B- and C-types) is quite acceptable. Moreover, deviation of the S-molecule axis, long or short, from the normal to anatase surface can even improve geometry, i.e., lower steric strain, since Ti−O−C angles decrease down to 130° while this declining increases up to the maximum of 45°. The last value corresponds to the rigid anchoring by three O−Ti bonds (E-type), or by four bonds (F-type), which are considered below.

Theoretically, there is another two-bond anchoring type (D-type, Figure 5c), when both COO groups of a bipyridyl are involved. However, realization of this anchoring type seems to be of a small probability. Noticably larger O···O spacings relative to the suitable Ti···Ti distance and the skewed orientation of Ti octahedrons toward the surface plane (Figure 5) result in either unacceptable trans- (O−Ti−O) angles (ca. 135° while Ti−O−C are 130−150°), or too large Ti−O−C angles (160−180°). The last could, in principle, increase up to indicated values, but it is doubtful that thermal energy can provide a transition to such state, at least at room temperature. In fact, the A→D transition is less probable than to B or C, because while one of the Ti−O−C bond angles has the usual value (initial A-type), the anchoring by the neighboring COO group becomes most unfavorable. The Ti−O distance also exceeds the valent bond length of ca. 2.0 Å. All that rejects the D-type anchoring.

The S-molecule in the B and C anchoring states retains considerable freedom of rotation around the axis passing through anchoring O atoms. Moreover, as was mentioned above, a tilting of the COO plane and consequently the whole molecule to the anatase surface even makes Ti−O−C angles closer to the optimal value of ca. 135°. So, a wide thermal rotation of the molecule around the indicated axis is to be expected, and just as the A→(B,C) transitions readily (and quickly) happen, the B→F or C→E transitions (Figure 6) must take place, if needed adsorption sites are not occupied. The bonding geometry of the E and F types is very good, and both types are most favorable thermodynamically. Using the E and F anchoring as the final products of the absorption process, we have built models of packing in the S-monolayer, based on the geometry considerations.

Possible Regular Packings in the S-Monolayer. In the absence of desorption, simultaneous formation of the E and F anchoring types leads inevitably to an irregular structure of the S-monolayer. Simulation of such structures is a very interesting problem, but is not the subject of this work. As to possible ordered structures, they are to consist of molecules with the same orientation. It is very unlikely in this case that an intermediate type of adsorption (B or C) is controlled by neighboring S-molecules.

The second most important condition for the existence of an ordered S-monolayer is the capability of adsorbed molecules to move along the surface. This condition, though weaker than the first one, is important due to the large dimensions of the S-molecule in relation to the spacing between the nearest absorption sites on the TiO_2 surface. It is clear that the smallest translation of $a = 3.78$ Å is taken here into account, since surface moving may go on without bonds' breaking only in that direction.

Keeping in mind these conditions, one can build ordered molecular packings of the S-monolayer, the closeness of which is restricted by the discrete distribution of anchoring sites over the anatase surface.

Three of the most dense packings for the E-type anchoring are shown in Figure 7. Two of them belong to the two-dimensional (2D) $P1$ space group, the third to the $P\bar{1}$ space group. To consider space groups of higher symmetry is meaningless because in this case a self-assembley process goes on by discrete steps with factual conservation of molecular orientation, which

(13) *Cambridge Structural Database*, Release 1997.

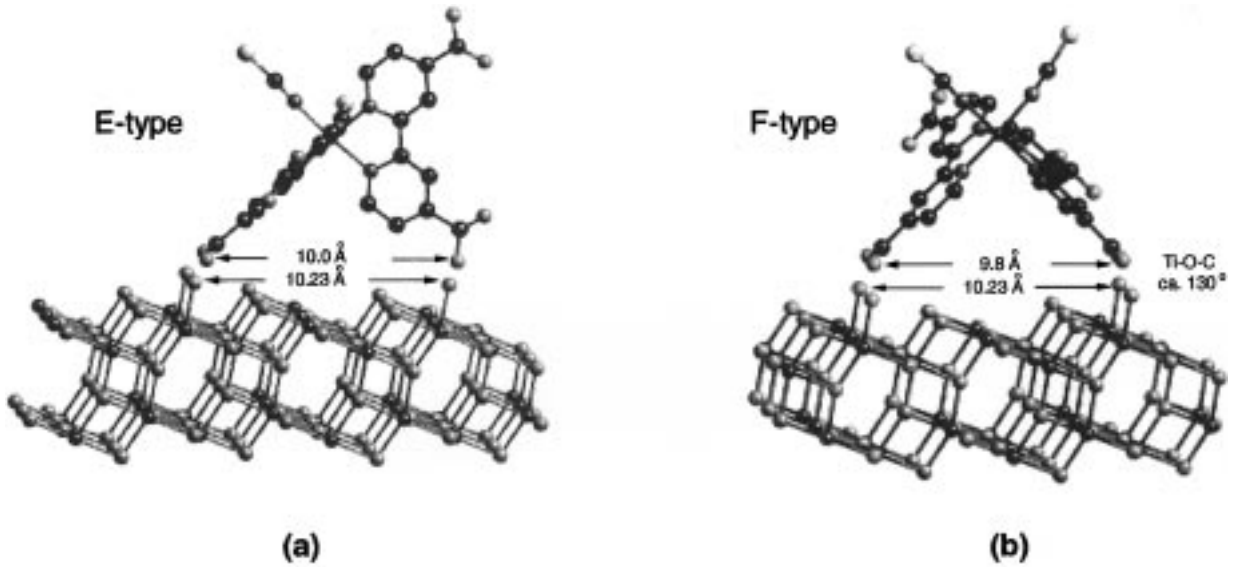

Figure 6. The most favorable, from the thermodynamics point of view, three-bond and four-bond types of anchoring.

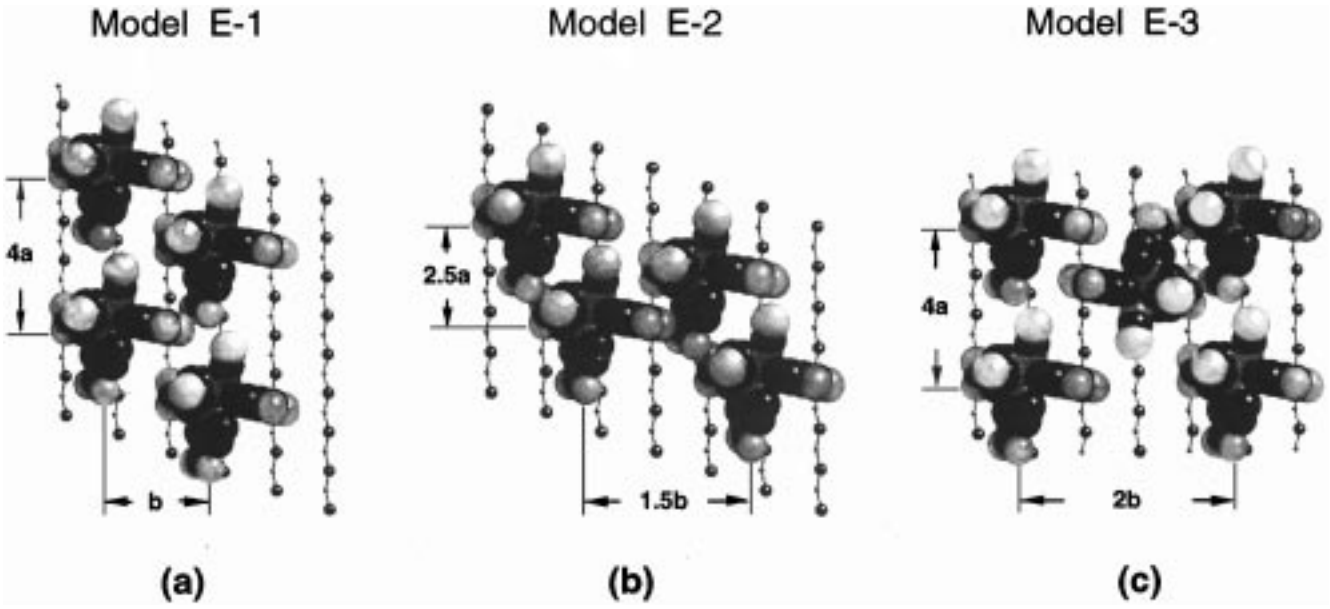

Figure 7. The most dense and lowest in symmetry ordered packings of S-monolayer for E-type of anchoring: (a,b) 2D space group $P1$, (c) 2D space group $P\bar{1}$ (here the unit cell contents and three nearest molecules are displayed, so the picture symmetry does not correspond to $P1$). A small overlapping in the E-2-model can be easily removed by minor rotations of COO groups.

prevents a real competition between different packings. Despite an evident thermodynamic advantage, the E-models are not to be particularly promising for an ordered S-monolayer. The point is that S-molecules in the E orientation do not possess C_2 symmetry in 2D sense.

Hence arrangements in Figure 5 are to be considered very specific. Each molecule can take two different orientations, whether it originates from C-type or A-type of anchoring, and the E-1 cluster of four molecules has the probability of formation equal to 0.125, not mentioning random **b** translations.

For F-models (Figure 8) molecular orientations should not be taken into account: due to the self-symmetry of the 2D inversion center, all the molecules have the same orientation, and the probability of formation of ordered packing is considerably higher. Nevertheless, the randomness of translations along the *b* axis strongly decreases this probability.

On the HRTEM patterns of the carefully prepared (101) cut anatase single-crystal sample coating with sensitizer **1** (precipitated from ethanol solution), moire patterns from overlapped fringes of thin sensitizer **1** crystal and the anatase (101) surface could be seen with the moire periodicity of 16.1 Å. The sensitizer interrow distances d_{hk} of approximately 12.2−12.6 Å for the models F-1 and F-3 (Table 3) could be compared with another value of $2d \sim 12.6$ Å obtained from moire patterns. The interference moire patterns of electron images from very thin single crystals of sensitizer and anatase were also discussed in the paper.[7]

Atomic Structure and Electron Transmittance of Interface. Simple Tight-Binding Model. The structural peculiarities of anatase and the sensitizer molecule have been obtained in the previous section. Now we will use these results to consider the electron transport from sensitizer molecule to anatase.

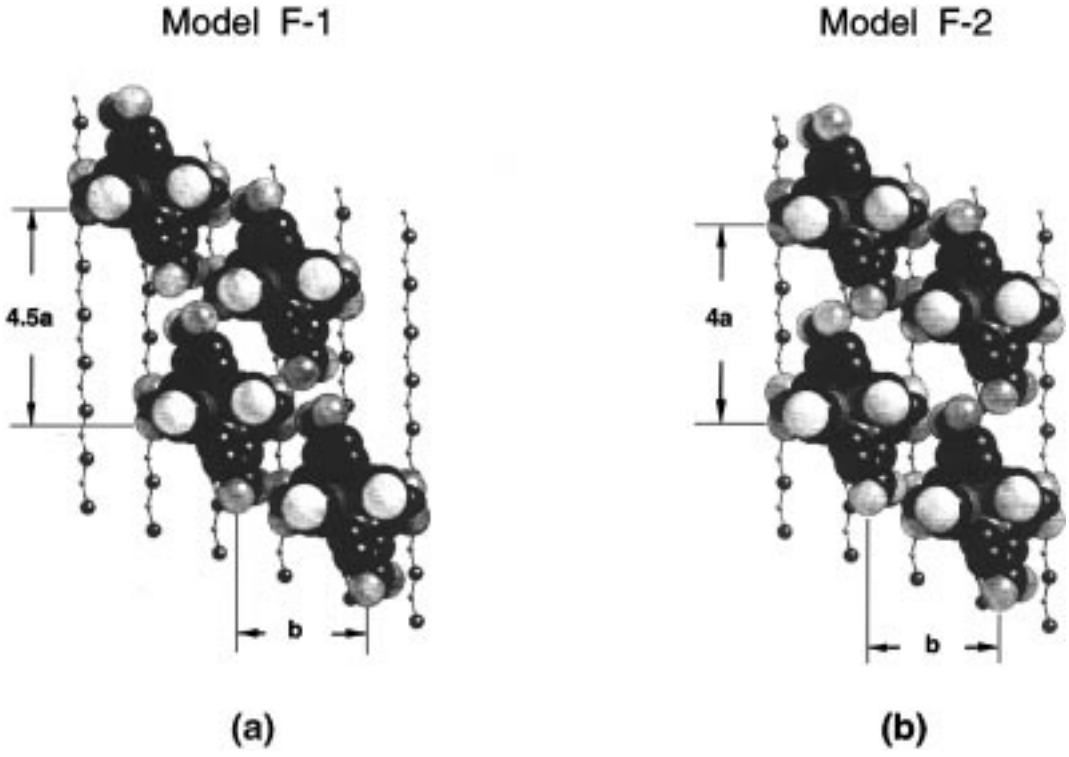

Figure 8. The most dense ordered packings for F-type anchoring (2D space group $P\bar{1}$). No overlapping is observed.

Table 3. Some Geometrical Parameters of S-monolayer Models for Sensitizer 1 on the Anatase Surface

		S-cell		
model	S-cell square (Å^2)	d_{hk}, Å	(hk)	Ru···Ti plane (Å)
E-1	155	12.2	(10)	
		10.2	(01)	
E-2	116	10.8	(10)	6.7
		7.1	(01)	
E-3	310	20.5	(10)	
	(two molecules)	15.1	(01)	
F-1	136	12.6	(10)	
		10.6	(01)	6.8
F-2	155	12.2	(10)	
		10.2	(01)	

Sensitizer (Figure 3) is a bulk molecule composed of a large number, $N \sim 40$, of a few different types of atoms. It is important that the size of the molecule essentially exceeds the spacing between neighboring atoms. Then it is possible to write the electron wave function as $\psi(\mathbf{r}) = \Sigma_{i,j} F_i(\mathbf{r})\phi_i(\mathbf{r}-\mathbf{a}_j)$, where $\phi_i(\mathbf{r}-\mathbf{a}_j)$ is the atomic wave function of the ith type of atom, which is situated at the site $\mathbf{r} = \mathbf{a}_j (j \le N, i \ll N)$, and $F_i(\mathbf{r})$ is a smooth function the mean size of which is on the order of the molecular size. The energy spectrum of the molecule should be composed of bands, which result from splitting of the appropriate atomic levels. The width of such bands is on the order of the hopping integral t between atoms (ca. 1 *eV*), and the spacing between neighboring levels in the band is about t/N.

It is interesting to consider the analogy between the sensitizer molecule and a doped semiconductor with a donor impurity. The light excites the electron from the Ru t_{2g} level to the "conduction band" of the anchoring ligand (π_L^+). Then the electron either leaves the molecule for the anatase via the Ti−O bond or comes back to the original Ru level accompanied by the photon emission. To make the solar cell more effective, we have to make the sensitizer/anatase interface be more transparent for the electron crossing.

Obviously, the single Ti−O bond between the sensitizer and anatase could not appreciably affect the electron states in each material. That is why we suppose that the electron states is known in each material. Then it is necessary to obtain the boundary conditions in order to match these states at the interface. For this reason the simple tight-binding model will be considered here.

It is clear from Figure 2 that the electron hopping along the Ti−O−Ti chain is the main mechanism of the charge transport from the surface (010) of anatase. The C−O bond connects the sensitizer molecule to anatase, whereas the oxygen atom belongs to both materials. This allows us to consider the simple tight-binding model presented by Figure 9c. Each Ti atom has two levels corresponded to the splitted 3d levels. The electron moves from the oxygen 2p level to one or another level of Ti. The C atom on the right-hand side belongs to a sensitizer molecule. The tight-binding equations for the TiO_2 chain are of the form

$$C_n^{O}(E - E_0) - t_1(C_n^{Ti_1} + C_{n-1}^{Ti_1}) - t_2(C_n^{Ti_2} + C_{n+1}^{Ti_2}) = 0 \qquad n < 0$$

$$C_n^{Ti_1}(E - E_1) - t_1(C_{n-1}^{O} + C_n^{O}) = 0 \qquad (1)$$

$$C_n^{Ti_2}(E - E_2) - t_2(C_{n-1}^{O} + C_n^{O}) = 0$$

Where C_n^{O}, C_n^{Ti1}, and C_n^{Ti2} are the probability amplitudes for the electron in the nth unit cell at the oxygen atom and the Ti level (1 and 2), respectively; E_0, E_1, and E_2 are the energies of those levels; t_1 and t_2 are the hopping integrals; and E is the electron energy.

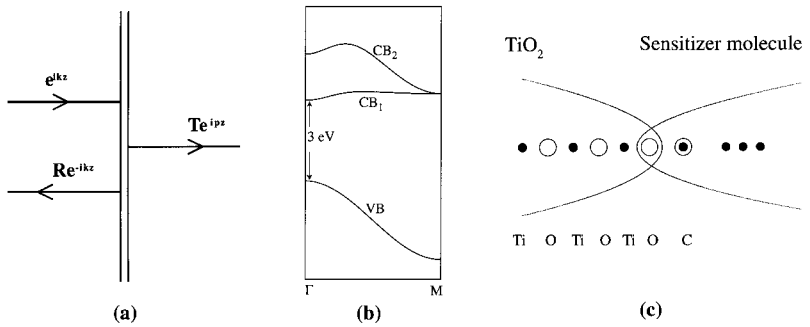

Figure 9. Structure of TiO_2/sensitizer interface and electron flux through it. (a) Electron transport through the interface. Arrowed lines schematically represent the incident, reflected, and transmitted parts of electron flux. (b) Simplified scheme of the TiO_2 band structure. Here CB_1 and CB_2 are the lowest conduction bands, and V is the top valence band. (c) Tight-binding one-dimensional model of TiO_2/sensitizer interface.

The eigenvalues ϵ_i of eq 1 correspond to the valence and two conduction bands of the electron spectrum. Assuming here $E_1 - E_0 = \Delta$, and $E_2 - E_1 = \delta \ll$e7 Δ, we find

$$\epsilon_0 = E_0 + \frac{4(t_1^2 + t_2^2)}{\Delta}\cos^2\frac{ka}{2}$$

for the valence band (V)

$$\epsilon_1 = E_1 + \frac{t_1^2}{t_1^2 + t_2^2}\delta$$

for the lower conduction band (CB_1)

$$\epsilon_2 = E_2 + \frac{t_2^2}{t_1^2 + t_2^2}\delta + \frac{4(t_1^2 + t_2^2)}{\Delta}\cos^2\frac{ka}{2} \quad (2)$$

for the upper conduction band (CB_2)

Equations 2 remarkably well reproduce the peculiarities of the TiO_2 band structure[14,15] in the $\Gamma - M$ direction (Figure 9b). It is important to emphasize the following: (1) the lower conduction band is almost flat in this direction, (2) minima of both conduction bands are at the Γ and M points of the Brillouin zone, and (3) the V and CB_2 bands are very similar in the vicinity of the M point. The Γ minima of both conduction bands also could be obtained from our model, if we introduce the direct electron hopping between titanium atoms. It is possible to do this because the real Ti−O−Ti chain looks like a zigzag with the bond angles of about 135°. However, this correction could not essentially affect the electron transport if the appropriate matrix element is small.[16] For agreement,[14] we assume $\delta = 0$, $\Delta \simeq 3$ eV, and $t_1^2 + t_2^2 = \hbar^2\Delta/2m_2a^2$, where $m_2 \simeq 3m_e$ is the effective mass at the edge of the upper conduction band.

To investigate the electron transport it is convenient to consider the envelope wave functions instead of the site amplitudes C_i. These envelopes, ψ_0, ψ_1, and ψ_2, are the plane waves; they obey the effective Schrödinger equations with the effective masses corresponding to the appropriate bands of the spectrum. It could be shown that $\varphi_0(z)$, $\varphi_1(z)$, and $\varphi_2(z)$, are the smooth functions of the z coordinate; they coincide with the amplitudes C_0, C_1, and C_2 when z coincides with the appropriate lattice site.

$$\varphi_0 = \psi_0$$

$$\varphi_1 = \frac{t_2}{\sqrt{t_1^2 + t_2^2}}\psi_1 + \frac{t_1}{\sqrt{t_1^2 + t_2^2}}\psi_2 e^{-i\pi z/a} \quad (3)$$

$$\varphi_2 = -\frac{t_1}{\sqrt{t_1^2 + t_2^2}}\psi_1 + \frac{t_2}{\sqrt{t_1^2 + t_2^2}}\psi_2 e^{-i\pi z/a}$$

To obtain the boundary conditions it is necessary to write the tight-binding equations for the boundary atoms. It is the oxygen atom in our case. In addition, the probability amplitude for the electron on the oxygen atom being expressed in terms of the TiO_2 envelopes can be expressed also in terms of the sensitizer wave function. Thus, we have

$$C_0^O(E - E_0) - t_1C_0^{Ti1} - t_2C_0^{Ti2} = tC_1^C$$

$$C_0^O = \psi^O(0)$$

We use eqs 1 and 3 in order to obtain the BC in the effective mass approximation

$$\Psi_2(0) = -\frac{at}{\hbar}\sqrt{\frac{2m_2}{\Delta}}\psi^C(c) + \frac{ia}{\hbar}\sqrt{2m_2\Delta}\psi^O(0)$$

$$\Psi'_2(0) = \frac{i}{\hbar}\sqrt{2m_2\Delta}\psi^O(0) \quad (4)$$

Where ψ^O and ψ^C are the wave functions of the electron in the sensitizer, and t is the hopping integral between the C and O atoms.

It is important that the second eq 4 connects the derivative $\Psi'_2(0)$ of the electron envelope in anatase with the sensitizer wave function at the oxygen. Whence $\psi^O(0) \sim \Psi_2(0)/(\lambda\sqrt{2m_2\Delta}/\hbar)$. Here $(2m_2\Delta/\hbar^2)^{-1/2} \simeq 2$Å, whereas the electron wavelength at the bottom of the CV_2 band of anatase λ is large. Existence of the small factor $(\lambda\sqrt{2m_2\Delta}/\hbar)^{-1}$ results in the essential supression [by $(\lambda\sqrt{2m_2\Delta}/\hbar)^2$ times] of the interface transmittance.[17] It is not the case only when the oxygen level

(14) Braginsky, L. S.; Romanov, D. A. *Fiz. Tverd. Tela* (St. Peterburg) **1995**, *37*, 2122 [*Sov. Phys. Solid State* **1995**, *37*].
(15) Glassford, K.; Chelikowsky, J. *Phys. Rev.* **1992**, *B46*, 1284.
(16) Braginsky, L. S.; Romanov, D. A. *Fiz. Tverd. Tela* (St. Peterburg) **1997**, *38*, 839 [*Sov. Phys. Solid State* **1997**, *39*].
(17) Zhu, Q.-G.; Kroemer, H. *Phys. Rev.* **1989**, *B27*, 3519.

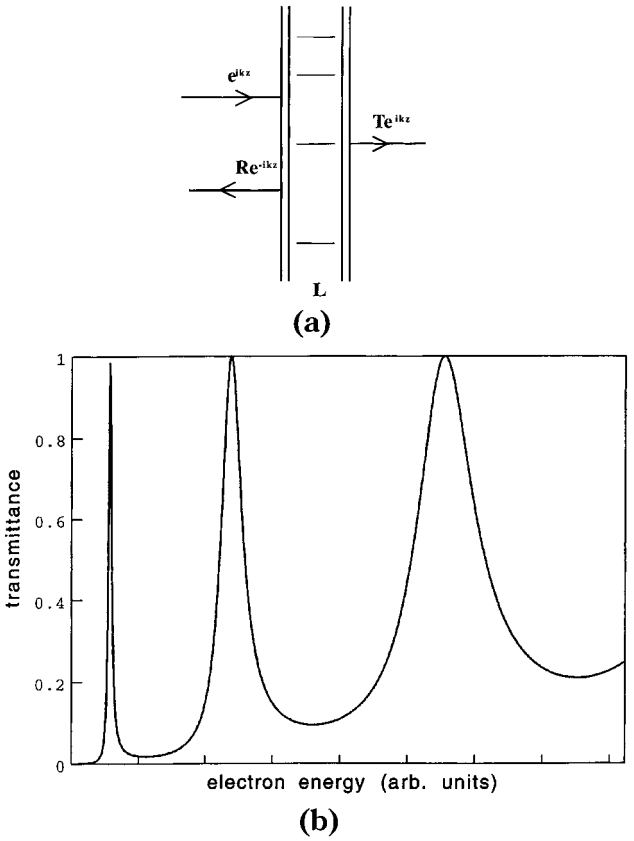

Figure 10. (a) Electron transport through a three-layer structure. Localized electron levels in the intermediate layer L are shown. (b) Transmittance of the three-layer structure as a function of incident electron energy.

comes close to the bottom of the anatase conduction band. The so-called structure resonance occurs in this case.

The following means may be proposed to increase the interface transmittance: (1) by adding or substituting the interface oxygen with some other atom in order to place the interface level close to the bottom of the anatase conduction band; (2) by implanting an intermediate layer (L) between the sensitizer and anatase. Indeed, if transmittance of each interface (molecule/L and $LTiO_2$) is small, then the energy spectrum of the electron in L is quantized. This means that only certain energy levels in L are available for an electron. The transmittance of the whole structure will be on the order of unity for the electrons, which energy coincides with these levels (Figure 10). This phenomenon is similar to the resonant tunneling of the electron through the localized level. It is possible to choose the parametes of L (e.g. its thickness and the material), so that the interface becomes transparent for electrons, with energies corresponding to the bottom of the sensitizer band; (3) by preparing a smooth interface. It is shown[3] that an interface can be considered as smooth if the effective parameters of the conduction CV2 band of anatase change to the band parameters of sensitizer on the distance of few lattice constants. The transmittance of such an interface is on the order of unity.

Conclusion

Based on the crystal structure data of the sensitizer S (Ru complex) and the substrate (TiO_2), different models of interactions of S are examined (A−F). Adsorption dynamics, including behavior of surface-fixed S-molecules, play a decisive role in formation of the S-monolayer. Thermodynamically, the F-models are much more favorable than the E-models and still more than the models with intermediate B- or C-type of anchoring. For the time being, there is no direct evidence of the superiority for one or another anchoring type. Some indirect comparison can be made via, e.g., measurements of monolayer density, the distance between Ru atoms and the surface plane of Ti atoms, and interrow spacings in the S-monolayer (Table 3). Taken together, these data allow a selection among possible packing models. In the case of a random structure or if the B and C anchoring types still can form a monolayer, simulation technique must be reexamined in more detail.

As to the influence of the atomic structure of TiO_2/sensitizer interface on electron injecting through it, calculations within our simple tight-binding model suggest more or less significant complications of this structure in order to enhance interface transparency. It is reasonable to consider such modifications with more concrete parameters of the model, including, e.g., specific data on electron spectra of sensitizer and possible "third material".

Acknowledgment. We are indebted to the Swiss Energy Office, Project EF-REN (91)054, and to the Swiss National Science Foundation, Project No. 7SUPJ048573, for financial support, to R. Wessicken (Solid State Physcis Department, Swiss Federal Institute of Technology) for help in HRTEM measurements, to Dr. M. Wörle (Laboratory of Inorganic Chemistry, Swiss Federal Institute of Technology) for X-ray data collection from the crystal **1**, to Dr. K. Kalyanasundaram for fruitful discussions, and to Prof. W. Steurer (Labor of Crystallography, Swiss Federal Institute of Technology) for his interest in this work.

Supporting Information Available: Bond lengths, bond angles, anisotropic displacement coefficients, calculated H atoms coordinates for **1** (5 pages); observed and calculated structure factors table (16 pages). Ordering information is given on any current masthead page.

CM980303G